

Plastics, Rubber and Composites

Macromolecular Engineering

ISSN: (Print) (Online) Journal homepage: www.tandfonline.com/journals/yprc20


Effect of surface modification and sodium dodecyl sulfate (SDS) on thermal properties of PMMA/SWCNT nanocomposites

Ersin Yanmaz & Mehmet Doğan


To cite this article: Ersin Yanmaz & Mehmet Doğan (2023) Effect of surface modification and sodium dodecyl sulfate (SDS) on thermal properties of PMMA/SWCNT nanocomposites, *Plastics, Rubber and Composites*, 52:9-10, 516-530, DOI: [10.1080/14658011.2023.2247732](https://doi.org/10.1080/14658011.2023.2247732)


To link to this article: <https://doi.org/10.1080/14658011.2023.2247732>

 View supplementary material 

 Published online: 18 Aug 2023.

 Submit your article to this journal 

 Article views: 162

 View related articles 

 View Crossmark data 

RESEARCH ARTICLE



Effect of surface modification and sodium dodecyl sulfate (SDS) on thermal properties of PMMA/SWCNT nanocomposites

Ersin Yanmaz^a and Mehmet Doğan ^b

^aDepartment of Chemical and Chemical Processing Technologies, Altinoluk Vocational School, Balıkesir University, Balıkesir, Turkey;

^bDepartment of Chemistry, Faculty of Science and Literature, Balıkesir University, Balıkesir, Turkey

ABSTRACT

In this study, the single-walled carbon nanotube (p-SWCNTs) and poly (methyl methacrylate) (PMMA) polymer nanocomposites were prepared by solution casting method. The effects of functionalization and sodium dodecyl sulfate (SDS) on the thermal properties of PMMA/p-SWCNT nanocomposites were investigated. Samples were characterised using BET, FTIR-ATR, SEM, DTA/TG, DSC, TEM and AFM. Morphological analyses showed that changes in the structure of SWCNTs with modification occurred and CNTs were tubular structure, homogeneously dispersed and nano-sized. Functionalised SWCNTs increased the first mass loss (T_{max1}), the second mass loss (T_{max2}) and glass transition temperatures (T_g) of PMMA. SDS assisted both better dispersion of CNTs and interaction between PMMA and CNTs. While PMMA/p-SWCNT-OH (0.1 wt.%) had the highest thermal stability in SDS-free medium, PMMA/SDS/p-SWCNT-O-APTS (0.1 wt.%) had the highest thermal stability in SDS medium. The maximum increases at T_{max1} and T_{max2} temperatures of nanocomposites were calculated as 49 and 13°C for PMMA/SDS/p-SWCNT-O-APTS (0.1 wt.%), respectively.

ARTICLE HISTORY

Received 1 March 2022

Revised 1 August 2023

Accepted 8 August 2023

KEYWORDS



SWCNT; PMMA; nanocomposite; functionalization; solution casting method; thermal properties


Introduction

Polymeric nanocomposites consisting of polymers reinforced with different nano-sized fillers such as bentonite [1], sepiolite [2], kaolin [3], perlite [4], hydroxyapatite [5], boron oxide [6], montmorillonite [7], etc are increasingly used in the defence industry, aerospace, automobile, sports and electronics industries due to their lightweight, high strength, high electrical and thermal conductivity. Today, one of the polymers commonly used in the areas mentioned above is poly(methylmethacrylate) (PMMA). It has excellent optical properties, balanced mechanical properties, good dielectric properties, weather resistance properties etc. Furthermore, it is also widely used in the building materials as it is cheap and easy to be processed [8]. However, PMMA has its shortcomings, such as low hardness, low wear resistance, heat resistance, especially low thermal performance. These properties of PMMA limit its application areas [9]. One way to improve these properties, especially thermal properties, of PMMA and expand its use areas is to prepare its nanocomposites with carbon nanotubes (CNTs).

Discovered by the Japanese scientist Iijima in 1991, CNTs [10] are considered a top class subject in academic research and various industrial fields. Because they have unique physical properties such as high

aspect ratio, good electrical conductivity, good mechanical strength and high thermal stability. These different properties of CNTs make them an excellent filling material in the polymer matrix [11]. CNT is a structure formed by rolling the graphite layer into a tubular structure. There are three types of CNT structures, namely single-walled carbon nanotube (SWCNT), double-walled carbon nanotube (DWCNT), and multi-walled carbon nanotube (MWCNT), according to the number of walls [12]. Despite these advantages of CNTs, they are poorly dispersed in the polymer matrix and/or in organic or aqueous solutions due to the van der Waals attractions between them. This can cause agglomeration of CNTs. The effective use of CNT is related to the homogeneous distribution in the polymer matrix. Dispersion of CNT samples in the PMMA matrix is the major problem to be solved for CNT reinforced polymer composites. It is seen in the literature that many studies focused on the improvement of the dispersion of CNTs in the polymer matrix or solvents and to prevent their agglomeration [13–15]. Methods such as surface treatment, chemical purification, solution mixing, melt blending, and polymerisation have been used in these studies [16–18]. Surface modification process to improve the physical and chemical properties of CNT samples allows a strong interaction between the polymer and CNT.

CONTACT Mehmet Doğan  mdogan@balikesir.edu.tr; mdogan7979@gmail.com  Department of Chemistry, Faculty of Science and Literature, Balıkesir University, Balıkesir 10145, Turkey

 Supplemental data for this article can be accessed online at <https://doi.org/10.1080/14658011.2023.2247732>.

© 2023 Institute of Materials, Minerals and Mining Published by Taylor & Francis on behalf of the Institute

Modification of CNT samples is important to fulfil the superior mechanical, electrical and biological functions of these materials and to increase their distribution in polymer matrices [19].

In our previous studies, we determined that the surface modification of CNT and solvent type in synthesis method were important in improving the thermal stability of poly (vinylacetate)/MWCNT, PMMA/MWCNT and PVA/SWCNT nanocomposites and the dispersion of CNTs in the polymer matrix [13,14,20]. Similar results were also found for PVA/MWCNT, epoxy/MWCNT, PVA/SWCNT nanocomposites [21–23]. These similar results revealed the importance of modification in improving the properties of nanocomposites.

In the literature, PMMA/SWCNT and PMMA/MWCNT nanocomposites were prepared using different methods and their mechanical, optical, electrical and thermal properties were investigated [24–26]. For example, Kalakonda and Banne synthesised PMMA/SWCNT nanocomposites using coagulation method. Optical and scanning electron microscopies showed an improved dispersion of SWCNTs in the PMMA matrix and comprehensive improvement in elastic modulus, electrical conductivity, and thermal stability with the addition of SWCNTs [27]. Ayanoglu and Doğan investigated the thermal degradation kinetics of PMMA/functionalised MWCNT nanocomposites and calculated the activation energies of nanocomposites in different solvent medium [20]. Ciobotaru et al. synthesised PMMA and modified SWCNT (SWCNT-COOH) composites using solvent dispersion method and investigated the thermal, mechanical and electrical conductivity properties of composites [28]. As can be seen from the literature summary above, there are many studies on the nanocomposite production of multi-walled carbon nanotubes with PMMA and other polymers. However, the number of studies on single-walled carbon nanotubes is quite limited. This is because the single-walled carbon nanotubes are not dispersed homogeneously in the polymer matrix due to the van der Waals attraction forces. To the best of our knowledge, there is no study the investigating the effects of functional groups and sodium dodecyl sulphate (SDS) on the thermal properties of PMMA/SWCNT nanocomposites. Thus, the aim of this study is to prepare PMMA/p-SWCNT nanocomposites by solvent casting method and to improve the thermal stability of PMMA. p-SWCNT is the purified SWCNT from SWCNT. For this, the surface of p-SWCNT was functionalised with hydroxyl and an organo silane compound to improve dispersion of SWCNT in PMMA matrix and solvent. In addition, SDS was added into the synthesis medium to provide homogeneous dispersion of p-SWCNT and the functionalised p-SWCNT samples into the PMMA matrix. PMMA, p-

SWCNT, the functionalised-p-SWCNT and their nanocomposites were characterised using Brunauer-Emmet-Teller (BET) surface area device, Fourier transform infrared-Attenuated total reflectance spectroscopy (FTIR-ATR), differential thermal analysis/thermogravimetry (DTA/TG), differential scanning calorimetry (DSC), atomic force microscopy (AFM), transmission electron microscopy (TEM) and scanning electron microscopy (SEM).

Experimental section

Materials

SWCNT with diameters of less than 1 nm, lengths of 1–3 μm , and carbon purities of >92% was purchased from Nanografi (Turkey); PMMA (M. W. = 35000 g/mol) from Acros Organics (Belgium); 3-aminopropyltriethoxysilane (APTS) from Merck Chemical Co. (Germany); N, N-dimethylformamide (DMF) and SDS from Sigma-Aldrich (Germany). All chemical reagents were of analytical grade and used as received without further purification.

Methods

Purification of SWCNT samples

HCl (100 mL, 5 M) and SWCNT (1 g) were placed into 250 mL reaction flask to increase the efficiency of SWCNT samples. After 1 h of ultrasonic bath at 30°C, it was stirred for 48 h (2 days) on a magnetic stirrer under reflux at 70°C. This mixture was filtered in a vacuum filtration device and washed with the purified water until pH = 7. After the filtrate was kept in an oven at 60°C for 24 h, it was dried at 60°C in a vacuum oven for 48 h. SWCNTs treated with HCl were named as p-SWCNT [29].

The hydroxylation of p-SWCNT

$\text{FeCl}_2 \cdot 4\text{H}_2\text{O}$ (0.3 M; 90 mL) and p-SWCNT (1 g) were placed into the reaction flask and dispersed in an ultrasonic bath for 1 h at 25°C. The mixture was taken on a magnetic stirrer and H_2O_2 (30%, 360 mL) was added dropwise. It was then stirred for 12 h at room temperature. After mixing, it was filtered with a vacuum filtration device. The filtrate was washed with HCl (5%) and with distilled water. The sample was dried for 24 h in an oven at 80°C and then for 48 h in a vacuum oven at 60°C. SWCNTs functionalised with $\text{Fe}^{2+}/\text{H}_2\text{O}_2$ (30%) were named as p-SWCNT-OH [30].

Functionalization of p-SWCNT-OH with APTS

p-SWCNT-OH (1 g), toluene (50 mL) and APTS (2 mL) were placed sequentially into the reaction flask. After dispersion in the ultrasonic bath for 0.5 h at room temperature, it was taken on a magnetic

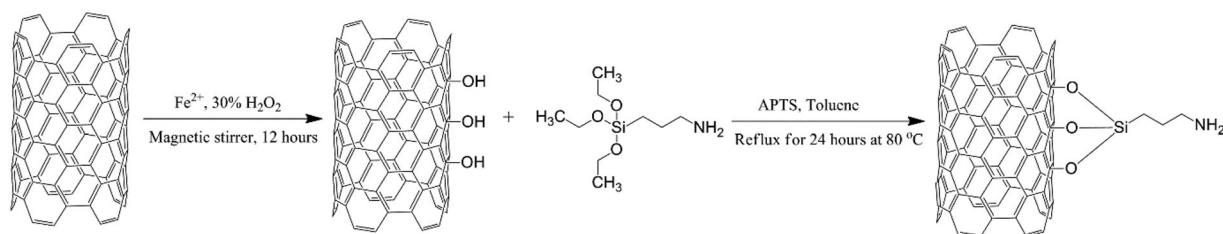


Figure 1. Surface functionalization reactions of *p*-SWCNT.

stirrer and refluxed (80°C, 24 h). Then, the mixture was filtered and washed with toluene, methanol and acetone, respectively. After washing, it was dried for 24 h in an oven at 80°C and for 24 h in a vacuum oven at 60°C. SWCNTs functionalised with APTS were named as *p*-SWCNT-O-APTS [14]. Synthesis of *p*-SWCNT-O-APTS from *p*-SWCNT is given in Figure 1.

Preparation of nanocomposites

PMMA/SWCNT nanocomposites (0.1, 0.5 and 1 wt.%) were prepared in DMF using solution casting method. The nanocomposite synthesis was conducted by following five steps: PMMA (1 g) and DMF (50 mL) were taken into a reaction flask and mixed on a magnetic stirrer for 1 h. DMF (50 mL) and SWCNT (0.1, 0.5 and 1 wt.%) were added into another reaction flask. The mixture was dispersed in an ultrahomogenizer for a total of 20, 5 min each time. PMMA solution and the dispersed SWCNT suspension were taken to ultrasonic bath set at 30°C and kept in ultrasonic bath for 2 h. After the polymer solution and the dispersed SWCNT suspension were combined, this mixture was kept in the ultrasonic bath for 2 h and then, mixed on the magnetic stirrer for 1 h. The solution was poured into a glass Petri

dish and placed in a drying-oven at 60°C to remove DMF. Subsequently, the material was taken into a vacuum oven with a temperature of 60°C and was kept for seven days. Thus, PMMA/*p*-SWCNT nanocomposites were prepared [28]. The same procedure was applied to prepare the other nanocomposites. The respective stages of nanocomposite preparation were clearly illustrated in Figure 2. SDS (1 wt.%) was added to the nanocomposite synthesis medium to increase the interactions between PMMA and SWCNT and to better disperse the SWCNTs in the PMMA matrix [31].

Characterisation of PMMA, SWCNTs and nanocomposites

Polymer, SWCNT samples and nanocomposites were characterised using FTIR-ATR, BET, DSC, DTA/TG, AFM, TEM and SEM. The specific surface areas of samples were determined by the nitrogen adsorption/desorption technique using a Quantachrome Nova2200e BET surface area instrument. Prior to the measurements, the samples were degassed at 100°C for 24 h and N₂ was used as the adsorbate gas. Infrared spectroscopy was used to investigate the interaction between polymer matrix and filler materials. FTIR measurement was carried out with PerkinElmer Spectrum 100 FTIR spectrometer in the wavenumber

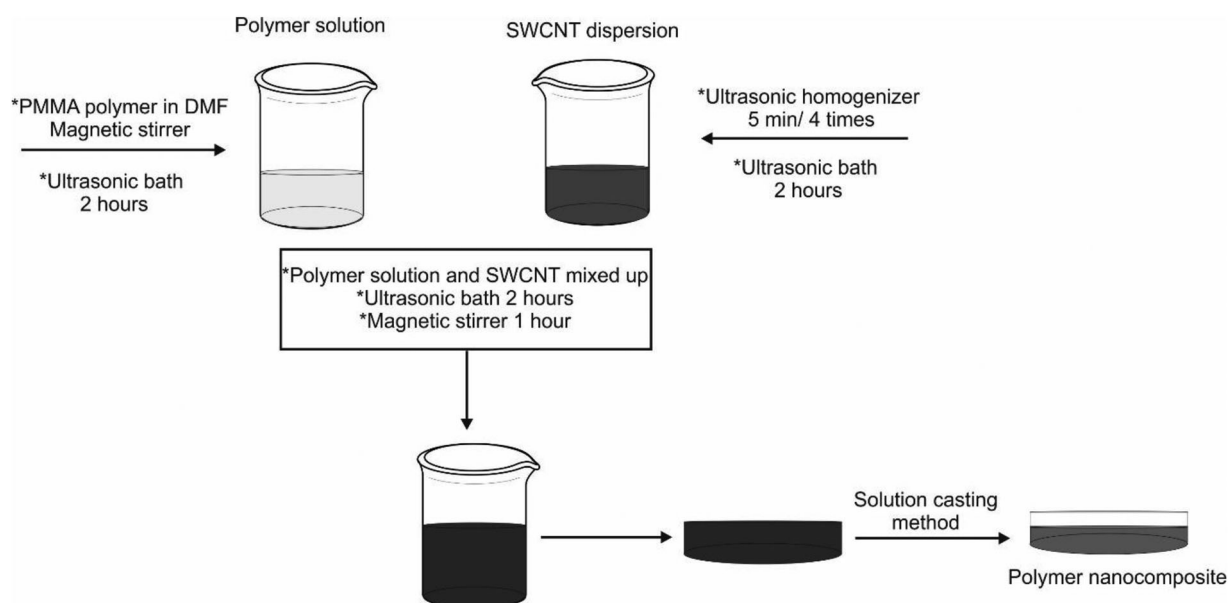


Figure 2. Experimental design of nanocomposite preparation method with solution casting method in SDS-free medium.

range of 4000–600 cm^{-1} . Thermogravimetric analysis of the samples were performed out using PerkinElmer Diamond simultaneous DTA/TG analyzer in the temperature range of 25°C–600°C with at heating rates of 10°C/min and flow of nitrogen gas is 200 mL/min. The glass transition temperatures (T_g) of the polymer and its nanocomposites were measured using the PerkinElmer DSC 4000 with a temperature range of 25°C–400°C at a heating rate of 10°C/min under nitrogen atmosphere. AFM topography of the prepared nanocomposites was obtained from a Nano-surf EasyScan 2 AFM Instrument in tapping mode (tip TAP190Al-G; vibration frequency 190 kHz) in air and room conditions. Maximum scanning size of the microscope probe was $25 \times 25 \mu\text{m}$. Morphological characterisation of the nanocomposites was examined by using the Zeiss Evo LS 10 Scanning electron microscopy (SEM). From the films, 1 mg/mL of sample and solvent were held and dispersed in the ultra-homogenizer for 5 min, and then one drop of the suspension was dropped onto the wafer. The sample was hold in a drying-oven for about 24 h to evaporate solvent. The study parameters were shown on SEM images.

TEM images of the modified SWCNT and nanocomposite samples were taken using JEOL JEM-1400 Plus transmission electron microscopy (taken at accelerating voltage 200 kV). The nanocomposites were suspended in DMF and a drop of the resulting mixture was placed on a carbon-coated Cu grid and dried in an oven.

Results and discussions

Characterisation

BET analysis

The changes in BET-specific surface areas of the SWCNT and functionalised SWCNTs may be a sign of modification. Specific surface areas of SWCNT, p-SWCNT, p-SWCNT-OH and p-SWCNT-O-APTS were measured as 510, 430, 360 and 60 m^2/g , respectively, using the Quantochrome Nova2200e BET device. BET surface areas of SWCNTs decreased with the purification and functionalization processes. Similar results were also found by different researchers. Cai et al. determined BET surface areas of SWCNT, manganese-terephthalic acid (Mn (TPA)) and Mn (TPA)-SWCNT as 668.61, 5.54 and 10.03 m^2/g , respectively [32]. In another study, BET surface areas of SWCNT, SWCNT + 4% Ni, SWCNT + 8% Ni and SWCNT + 12% Ni samples were measured as 584.8, 520.8, 478.6 and 436.0 m^2/g , respectively. In both studies, BET surface area of SWCNT decreased with modification [33]. The variation in surface areas of SWCNT, p-SWCNT and functionalised SWCNTs is quite compatible with the literature. The

decreasing of BET surface area with purification and functionalization may be due to the deformation of SWCNT structure, the occurrence of structural defects and the blocking of the ends of the tube with modifiers [34–37].

FTIR analysis

Figure 3 illustrates FTIR-ATR spectra of PMMA, p-SWCNT, functionalised-SWCNT and their nanocomposites. It can be seen from FTIR spectra that p-SWCNT has been successfully functionalised. Generally, the bands observed at 1257, 1453 and 1167 cm^{-1} are related to C–O–C, C–OH and C–O oxygen-containing functional groups, respectively; the band observed between 1600–1650 cm^{-1} to the C–C skeleton; and the band observed around 1730 cm^{-1} to the carbonyl group (or carboxylic acid and ester) [38]. When the spectrum of p-SWCNT is examined (Figure 3(a)), the C–C band is seen at 1633 cm^{-1} and C–H band at 2919 and 2841 cm^{-1} . The most important functional group of PMMA is the carbonyl or ester group. Figure 3 shows the main FTIR bands of PMMA. The band belonging to the carbonyl group was observed at 1723 cm^{-1} , the C–H stretching vibration bands of the $-\text{CH}_3$ and $-\text{CH}_2$ groups at 2991 and 2950 cm^{-1} , the C–H bending vibration band of the $-\text{CH}_3$ group at 1386 cm^{-1} , the vibration bands of the C–H group at 1386 and 750 cm^{-1} , and the peaks of the C–O–C single bond bending vibrations between 986 and 841 cm^{-1} [28,39]. FTIR-ATR spectra of PMMA/p-SWCNT nanocomposites were shown in Figure 3(a).

The p-SWCNT was hydroxylated by Fenton reaction and the p-SWCNT-OH structure was obtained. FTIR-ATR spectrum of p-SWCNT-OH was given in Figure 3(b). In this spectrum, the wide and intense hydroxyl vibration band between 3000–3500 cm^{-1} (3425 cm^{-1}), C–H stretching vibration bands at 2928 and 2854 cm^{-1} and C–C band at 1635 cm^{-1} are seen. When Figure 3(a and b) are compared, the 2919, 2841 and 1633 cm^{-1} bands of p-SWCNT shifted to 2928, 2854 and 1635 cm^{-1} , respectively. These band shifts and the hydroxyl band of p-SWCNT-OH in Figure 3(b) are evidences of hydroxylation of p-SWCNT. In the spectrum of nanocomposites, it was determined that some bands of PMMA shifted to higher and lower wave numbers. These band shifts are an indicative of interactions between PMMA and p-SWCNT-OH.

As a result of the reaction of p-SWCNT-OH with APTS, p-SWCNT-O-APTS was obtained. The FTIR-ATR spectrum of this reaction was shown in Figure 3(c). The absence of the hydroxyl peak of p-SWCNT-OH in this spectrum is a proof of synthesis of p-SWCNT-O-APTS. Also, new bands have appeared in the spectrum of p-SWCNT-O-APTS in Figure 3(c), different from those of p-SWCNT and

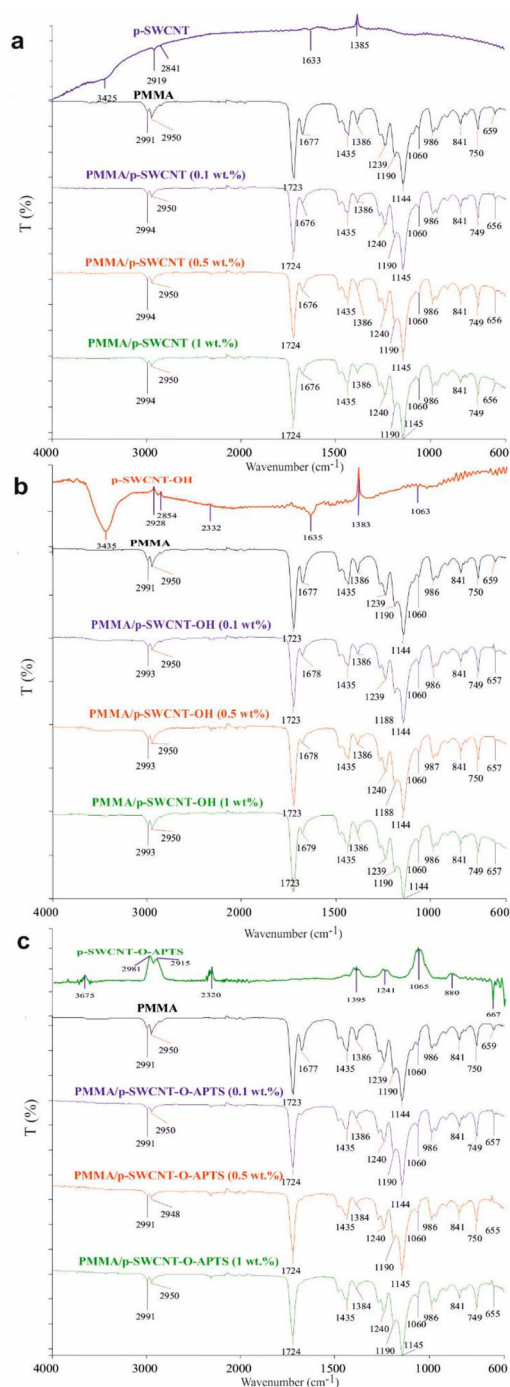


Figure 3. FTIR-ATR spectrum of (a) PMMA/p-SWCNT, (b) PMMA/p-SWCNT-OH and (c) PMMA/p-SWCNT-O-APTS nanocomposites.

p-SWCNT-OH. The bands at 1065, 1241, 1395 and 3400 cm^{-1} originate from the bands of Si-O, CH_2 -wagging, Si- CH_2 and free $-\text{NH}_2$ groups in the structure of p-SWCNT-O-APTS, respectively [40–43]. Yang et al. showed that the bands at 2920 and 2850 cm^{-1} corresponded to C-H bonds of alkyl and alkoxy groups in APTS, the band at 1116 cm^{-1} to the asymmetrical stretching vibration of the Si-O-R bond, and the weak band at 1456 cm^{-1} to the bending vibration of the N-H bond in aminosilane [44]. In another study, Su et al. observed that the bands at

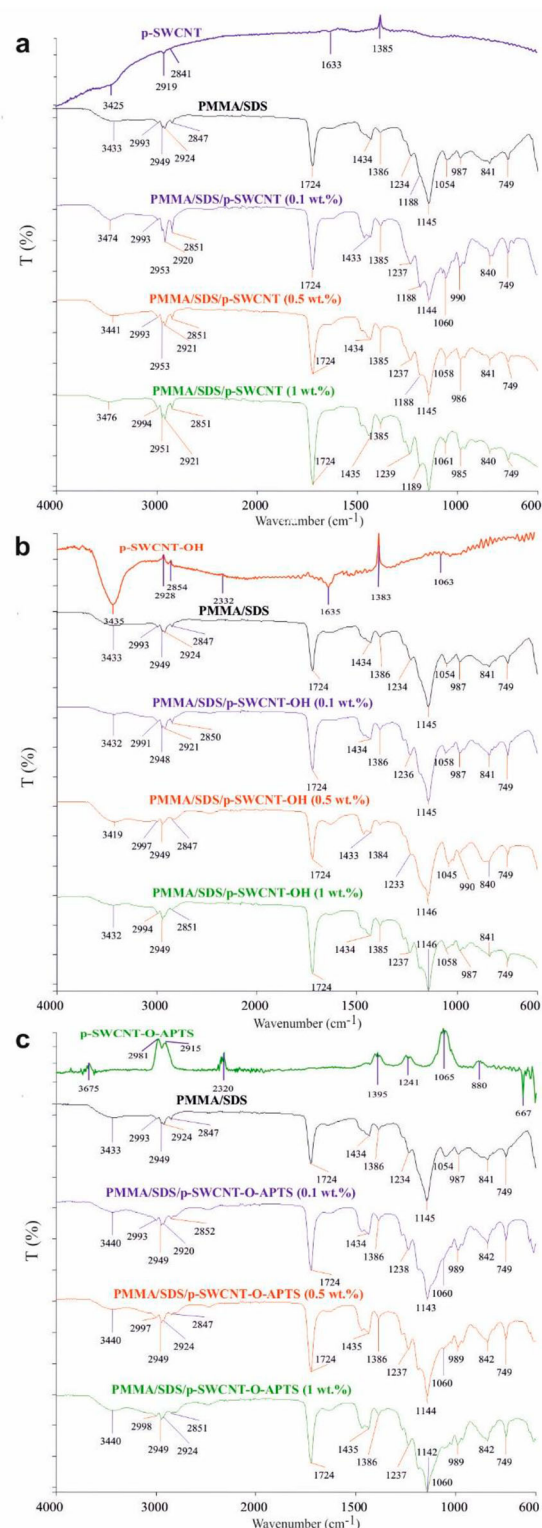


Figure 4. FTIR-ATR spectrum of (a) PMMA/SDS/p-SWCNT, (b) PMMA/SDS/p-SWCNT-OH and (c) PMMA/SDS/p-SWCNT-O-APTS nanocomposites.

3370 , 2950 , 1600 and 1030 cm^{-1} were related to the vibrations of N-H and N-H_2 , C-H₂, N-H and Si-O-Si, respectively [45]. In nanocomposites, the carbonyl band of PMMA at 1723 cm^{-1} shifted to 1724 cm^{-1} , and the C-H bands at 1386 and 750 cm^{-1} shifted to 1384 and 749 cm^{-1} .

Figure 4 shows the FTIR-ATR spectrum of the synthesised nanocomposites by adding SDS. The FTIR-

ATR spectra do not differ significantly from those in Figure 3. However, with the addition of SDS, it was seen that the intensity of some peaks belonging to the alkyl groups increased and a new peak belonging to the sulfate group emerged. For example, the asymmetric and symmetric CH_3 and CH_2 bands appear at 2924 and 2847 cm^{-1} in the FTIR spectrum of PMMA/SDS. In addition, a band belonging to the symmetrical sulfate group was seen at 1054 cm^{-1} [46]. Shifts in these peaks were also observed in PMMA/SDS/p-SWCNT nanocomposites.

SEM, TEM and AFM analysis

In Figure 5, the SEM images of PMMA/p-SWCNT (0.1, 0.5 and 1 wt.%), PMMA/p-SWCNT-OH (1 wt.%) and PMMA/p-SWCNT-O-APTS (1 wt.%) nanocomposites were given at 5.000 and 10.000 magnifications. It is seen that CNT samples are uniformly dispersed without agglomerate in the polymer matrix. Figure 6 illustrates TEM images of the purified and functionalised CNTs. SWCNT samples are in nano size and tube morphology. The morphologies of p-SWCNT and the functionalised SWCNTs are different from each other. There is no change in the diameter and length of the samples. However, point and sphere-like structures appear on the surface of the functionalised samples. This may be due to changes in the structure of p-SWCNT as a result of hydroxylation and silylation reactions. These results support FTIR-ATR analyses. TEM images of PMMA/p-SWCNT-OH (1 wt.%) and PMMA/p-SWCNT-O-APTS (1 wt.%) were given in Figure 6(d and e). Again, it can be said that SWCNT nanoparticles are dispersed in nano-sized and homogeneously in the PMMA matrix, and SWCNT nanoparticles are tubular structure [47].

Surface roughness is one of the important morphological properties of materials, and surface roughness value is a good indicator of the performance properties of the mechanical components of materials. Roughness plays an important role in determining how a material will interact with its environment. Both profile and area roughness parameters can be calculated from AFM topographies. 2D and 3D AFM topographies of PMMA/p-SWCNT (0.1, 0.5 and 1 wt.%), PMMA/p-SWCNT-OH (1 wt.%) and PMMA/p-SWCNT-O-APTS (1 wt.%) illustrate in Figure 7 with surface scanning results of $25 \times 25 \mu\text{m}^2$. Profile and area roughness parameters of PMMA/p-SWCNT (0.1, 0.5 and 1 wt.%), PMMA/p-SWCNT-OH (1 wt.%) and PMMA/p-SWCNT-O-APTS (1 wt.%) were given in Table 1. Surface roughness of PMMA/p-SWCNT nanocomposites increases with increasing amount of p-SWCNT. PMMA/p-SWCNT (0.5 wt.%) nanocomposite has the highest surface roughness. Among nanocomposites containing 1 wt.% SWCNTs, the nanocomposite with the highest surface roughness

is PMMA/p-SWCNT, followed by PMMA/p-SWCNT-OH and PMMA/p-SWCNT-O-APTS, respectively. In general, these results show that functionalization is an important chemical process in reducing surface roughness [7,48,49].

TG and DSC analysis

Thermal gravimetric analysis of SWCNTs

Thermal gravimetry studies give important information about the temperature-depending mass losses of the samples. In this study, since p-SWCNTs were modified with different functional groups, the changes in the mass losses of the samples can be accepted as a sign of modification. Figure 8 shows the TG thermograms of both CNT samples and their nanocomposites. As can be seen from the figures, the mass losses of CNTs increase with modification. The mass loss of p-SWCNT is 6 wt.%, while the mass losses of p-SWCNT-OH and p-SWCNT-O-APTS are 13 and 24 wt.%, respectively. The higher mass loss of p-SWCNT-O-APTS is due to its higher molecular weight of the APTS molecule functionalised on CNT surface compared to OH group. The low decrease in mass losses of p-SWCNT and the functionalised p-SWCNTs in the studied temperature range is an indication of the high thermal stability of these materials [50].

Thermal gravimetric analysis of nanocomposites

T_x represents the temperature at which x wt.% mass loss occurs and T_{max} represents the degradation temperatures of the sample. Figure 8 shows the TG thermograms of PMMA and its nanocomposites. In these thermograms, PMMA decomposes in two steps. The first mass loss was in the temperature range of 174–229°C ($T_{\text{max}1} = 213^\circ\text{C}$). The mass loss in this step was about 8.1 wt.%. Reasons for this mass loss may be due to i. the removal of moisture absorbing in the pores and structure of PMMA, ii. the solvent that cannot be completely removed from the structure during the synthesis of PMMA, and iii. thermal degradation of the unsaturated bonds at the ends of the molecular chains of PMMA [51]. The second mass loss was in the temperature range of 358°C–405°C ($T_{\text{max}2} = 385$) and the mass loss in this step was about 91.2 wt.%. The mass loss is caused by the random fracture of the C–C bond of the main PMMA chains [52]. The amount of residual at 600°C is 0.2 wt.%. Similar results were found by Nikolaidis and Achilias [53], Gao et al. [54] and Kausar [55]. They determined that PMMA degraded in two steps. However, slight variations were observed in T_{max} temperatures. The reason for this may be the molecular weight and synthesis method of PMMA, and impurities in the structure of PMMA [20,56].

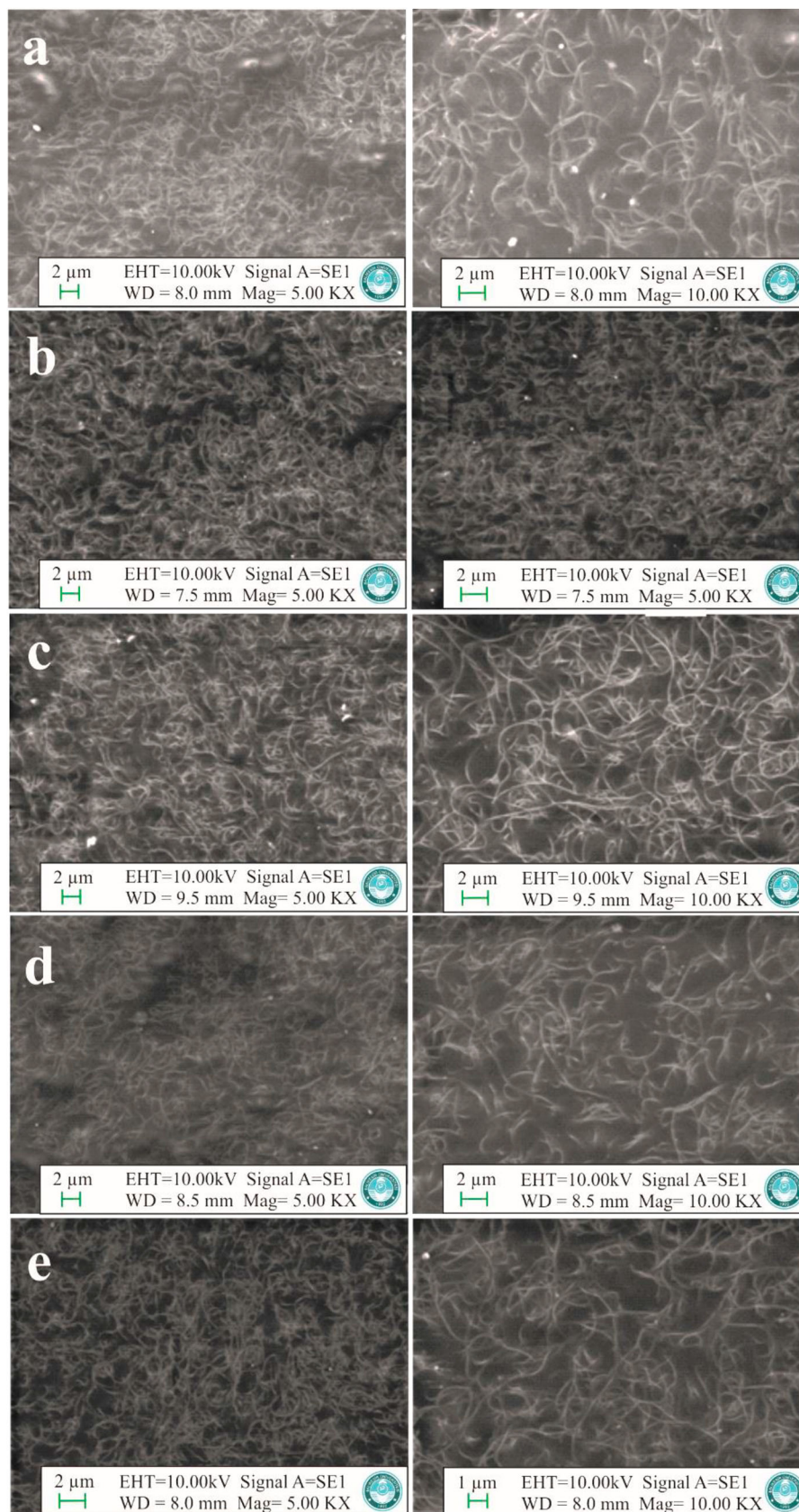


Figure 5. SEM images of (a) PMMA/p-SWCNT (0.1 wt.%), (b) PMMA/p-SWCNT (0.5 wt.%), (c) PMMA/p-SWCNT (1 wt.%), (d) PMMA/p-SWCNT-OH (1 wt.%) and (e) PMMA/p-SWCNT-O-APTS (1 wt.%) nanocomposites.

TG thermograms of PMMA/p-SWCNT, PMMA/p-SWCNT-OH and PMMA/p-SWCNT-O-APTS nanocomposites were given in Figure 8(a–c). Similar to PMMA, nanocomposites degrade in two steps.

However, there are differences in T_{\max} and T_x temperatures and residual amounts calculated from thermograms of PMMA and its nanocomposites (Table 2). Among PMMA/p-SWCNT nanocomposites, the

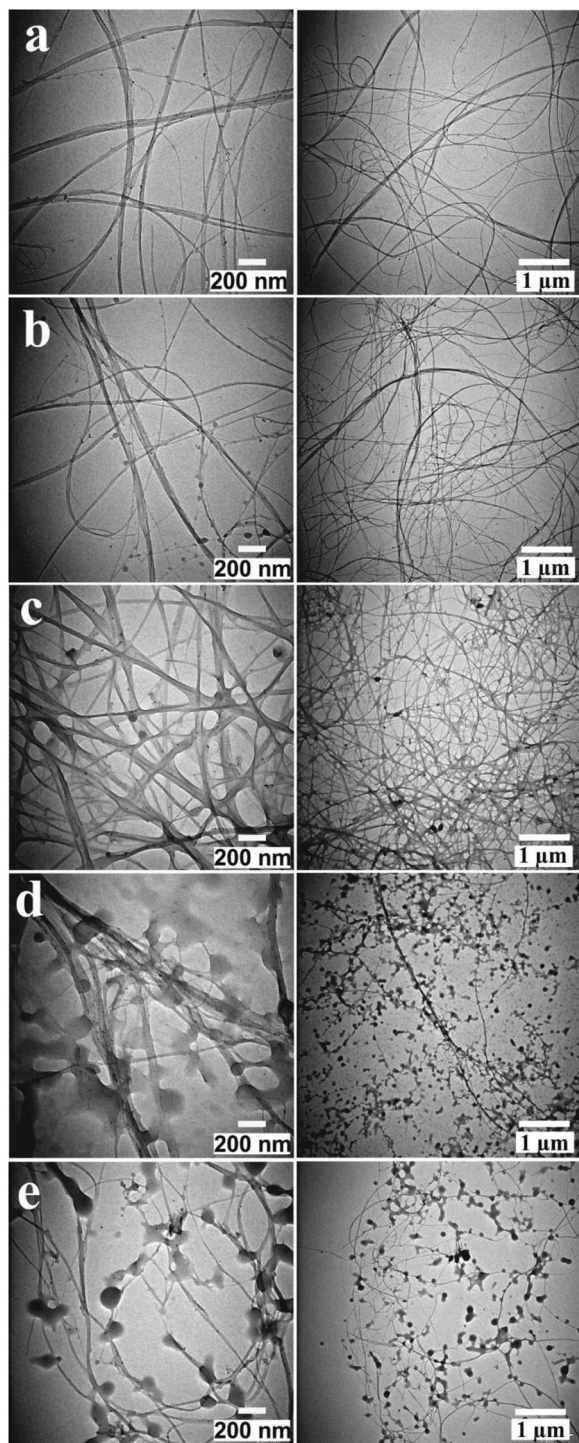


Figure 6. TEM images of SWCNTs and PMMA nanocomposites: (a) p-SWCNT, (b) p-SWCNT-OH, (c) p-SWCNT-O-APTS, (d) PMMA/p-SWCNT-OH (1 wt.%) and (e) PMMA/p-SWCNT-O-APTS (1 wt.%).

sample with the highest thermal stability was determined as PMMA/p-SWCNT (0.1 wt.%). With the increase of the p-SWCNT amount of the nanocomposite, T_x values first increased and then decreased. T_{10} and T_{80} temperatures of PMMA was calculated as 291°C and 395°C, respectively, while T_{10} and T_{80} temperatures for PMMA/p-SWCNT (0.1 wt.%) nanocomposite was calculated as 324 and 398 °C. The increase in T_{10} temperature of nanocomposite is considerably higher than T_{80} temperature. T_{max1} and

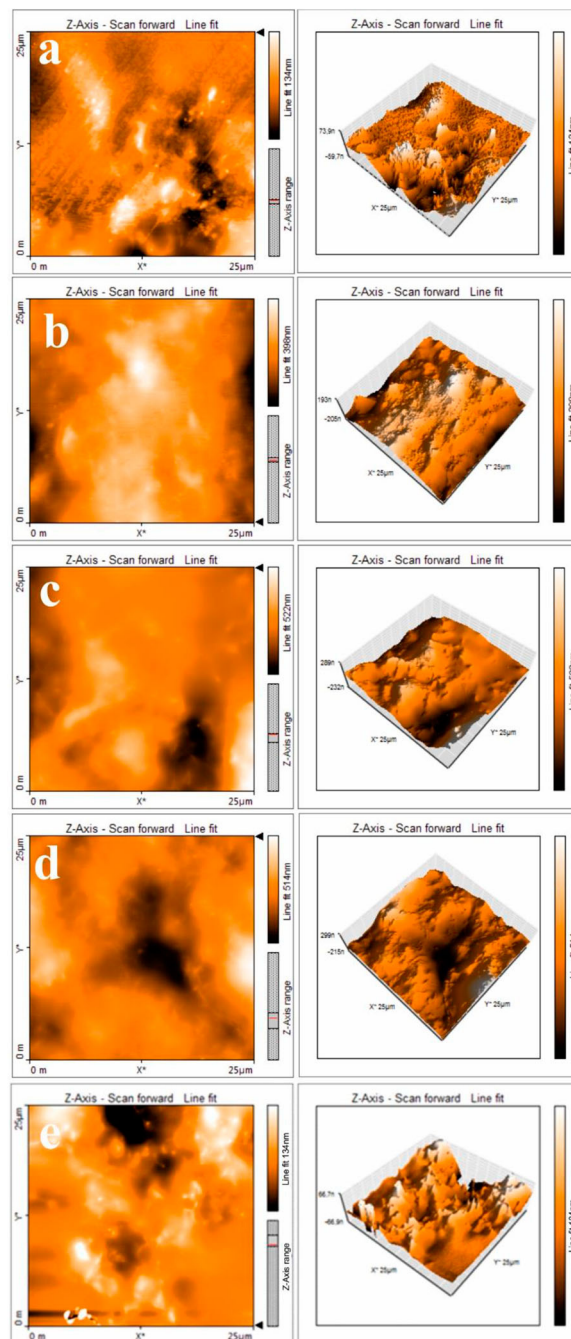


Figure 7. Two-dimensional and three-dimensional AFM analysis: (a) PMMA/p-SWCNT (0.1 wt.%), (b) PMMA/p-SWCNT (0.5 wt.%), (c) PMMA/p-SWCNT (1 wt.%), (d) PMMA/p-SWCNT-OH (1 wt.%) and (e) PMMA/p-SWCNT-O-APTS (1 wt.%) nanocomposites.

Table 1. Profile and area roughness parameter values of PMMA nanocomposites.

Nanocomposites	R_a	R_q	S_a	S_q
PMMA/p-SWCNT (0.1 wt.%)	16.3	20.6	16.4	21.8
PMMA/p-SWCNT (0.5 wt.%)	56.6	66.8	55.9	67.9
PMMA/p-SWCNT (1 wt.%)	50.8	62.5	57.4	76.2
PMMA/p-SWCNT-OH (1 wt.%)	51.7	60.2	56.2	75.3
PMMA/p-SWCNT-O-APTS (1 wt.%)	16.7	20.7	17.9	26.4

T_{max2} temperatures are 213°C and 385°C for PMMA, while it is 151°C and 387°C for PMMA/p-SWCNT (0.1 wt.%) nanocomposite. The decrease in T_{max1}

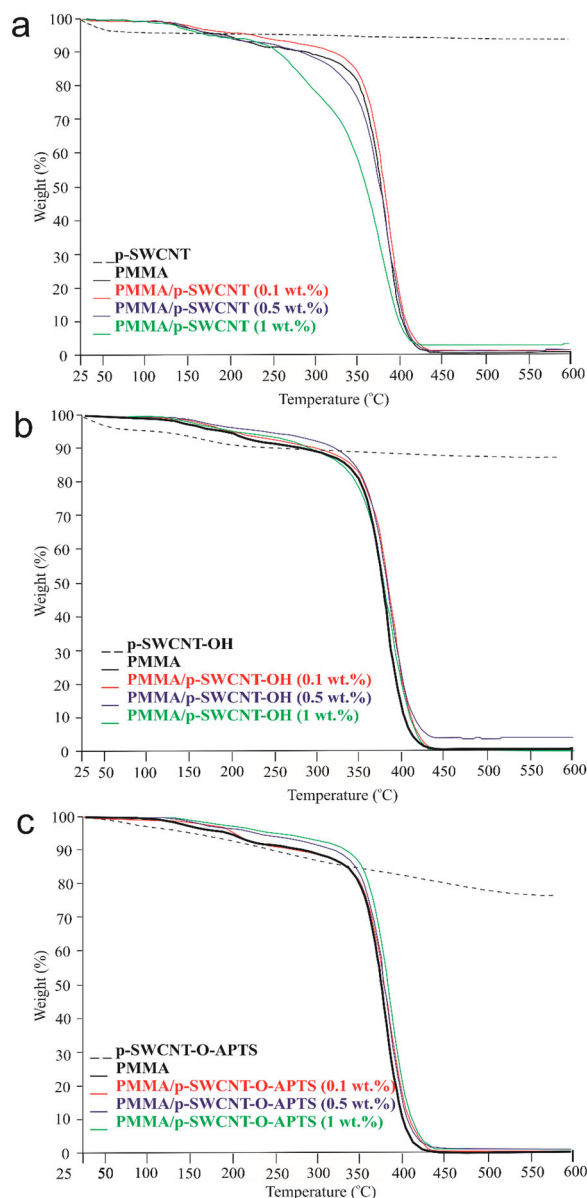


Figure 8. TG thermograms of (a) PMMA/p-SWCNT, (b) PMMA/p-SWCNT-OH and (c) PMMA/p-SWCNT-O-APTS nanocomposites.

temperature is probably due to solvent and impurities in the structure of nanocomposite. Moreover, the residual amount of all nanocomposites increased with the increasing amount of filling. The sample with the highest thermal stability among PMMA/p-SWCNT-OH nanocomposites is PMMA/p-SWCNT-OH (0.1 wt.%). $T_{\max 1}$ and $T_{\max 2}$ temperatures were determined as 230°C and 390°C, while T_{10} and T_{80} temperatures were determined as 318°C and 401°C. Compared to PMMA, increases of 27°C, 6°C, 17°C and 5°C occurred in $T_{\max 1}$, $T_{\max 2}$, T_{10} and T_{80} temperatures, respectively. It was also observed that the amount of residual increased when the amount of filling increased. The increase in thermal stability may be due to hydrogen bonds formed between the carbonyl group of PMMA and the hydroxyl group of p-SWCNT-OH. SEM images show that p-SWCNT-OHs are not agglomerated

and are uniformly dispersed in the PMMA matrix. This homogeneous distribution can lead to increased hydrogen bonds between PMMA and CNTs. Therefore, it can be said that the nanocomposite exhibits higher thermal stability. Among the PMMA/p-SWCNT-O-APTS samples, the nanocomposite with the highest thermal stability is PMMA/p-SWCNT-O-APTS (0.1 wt.%). Compared to PMMA, increases of 5°C, 2°C and 6°C occurred in $T_{\max 1}$, $T_{\max 2}$ and T_{80} temperatures, while a decrease of 6°C in T_{10} temperature was observed. The residual amount of nanocomposites increased with increasing amount of filling.

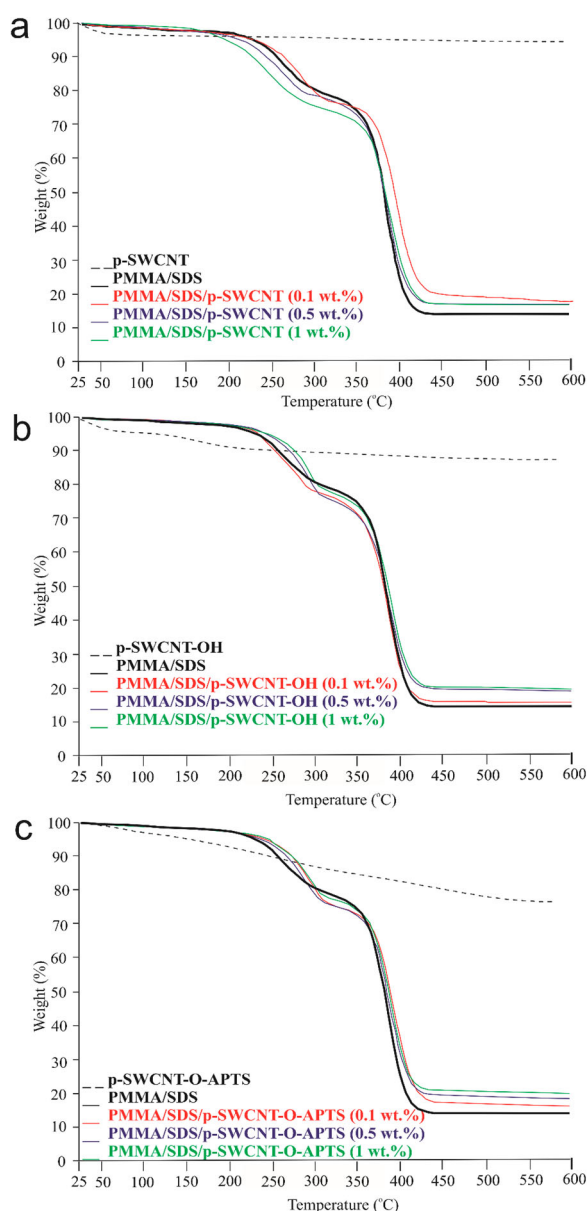
From the above results, the nanocomposites with the highest thermal stability among all nanocomposites were determined as samples containing 0.1 wt.% CNT. This shows that the CNTs are more homogeneously dispersed between the polymer chains at low ratios, but they are not effectively dispersed or partially agglomerated between the polymer chains due to the van der Waals interactions between CNTs at high ratios. As a result, the thermal stability of nanocomposites with high CNT ratios will be low. The sample with the highest thermal stability among all nanocomposites is PMMA/p-SWCNT-OH (0.1 wt.%). p-SWCNT does not have any functional groups. However, p-SWCNT-O-APTS has an amine containing organo silane group. The steric effect is an important factor in the interaction of bulky molecules. Although p-SWCNT has the highest thermal stability among CNT samples, its interaction with PMMA is very limited since it does not have any functional groups in its structure. Therefore, the thermal stability of its nanocomposites is lower than that of p-SWCNT-OH. p-SWCNT-OH has lower thermal stability than p-SWCNT. However, the thermal stability of its nanocomposites is higher because the hydroxyl functional group in its structure forms hydrogen bonds with the carbonyl group of PMMA. As can be seen from Table 2, both T_x and T_{\max} temperatures of PMMA/p-SWCNT-OH (0.1 wt.%) nanocomposite are higher than those of other nanocomposites. In addition, it can be said that the steric effect is not important in the interaction of the hydroxyl group of p-SWCNT-OH with the carbonyl group of PMMA. The thermal stability of nanocomposites of p-SWCNT-O-APTS is higher than nanocomposites of p-SWCNT but lower than p-SWCNT-OH nanocomposites. p-SWCNT-O-APTS is the most thermally unstable filler. However, it has an amine-containing organo silane group in its structure. The amine group of this structure and the carbonyl group of PMMA can form hydrogen bonds. However, it can be said that the interaction will be low due to difficulties in orienting the amine containing organo silane group of p-SWCNT-O-APTS in a sterically suitable geometry to form hydrogen bond with the

Table 2. Data obtained from DTA/TG and DSC thermograms for PMMA and its nanocomposites.

Samples	T ₁₀ (°C)	T ₈₀ (°C)	T _{max1} (°C)	T _{max2} (°C)	Residue(%)	T _g (°C)
PMMA	291	395	213	385	0.2	88
PMMA/p-SWCNT (0.1 wt.%)	324	398	151	387	0.5	96
PMMA/p-SWCNT (0.5 wt.%)	288	396	171	384	1.2	97
PMMA/p-SWCNT (1 wt.%)	261	389	154	378	2.8	99
PMMA/p-SWCNT-OH (0.1 wt.%)	318	401	230	390	0.2	100
PMMA/p-SWCNT-OH (0.5 wt.%)	325	401	168	390	3.7	105
PMMA/p-SWCNT-OH (1 wt.%)	319	399	169	383	2.2	104
PMMA/p-SWCNT-O-APTS (0.1 wt.%)	285	401	218	387	0.4	90
PMMA/p-SWCNT-O-APTS (0.5 wt.%)	326	399	160	387	1.4	100
PMMA/p-SWCNT-O-APTS (1 wt.%)	338	403	198	386	1.4	100
PMMA/SDS	263	410	256	385	14.1	94
PMMA/SDS/p-SWCNT (0.1 wt.%)	265	443	285	395	17.6	92
PMMA/SDS/p-SWCNT (0.5 wt.%)	250	416	270	392	16.5	110
PMMA/SDS/p-SWCNT (1 wt.%)	235	420	245	393	16.7	111
PMMA/SDS/p-SWCNT-OH (0.1 wt.%)	258	411	286	388	15.7	95
PMMA/SDS/p-SWCNT-OH (0.5 wt.%)	275	430	297	389	19.1	107
PMMA/SDS/p-SWCNT-OH (1 wt.%)	281	440	297	393	19.6	99
PMMA/SDS/p-SWCNT-O-APTS (0.1 wt.%)	280	425	305	398	16.6	94
PMMA/SDS/p-SWCNT-O-APTS (0.5 wt.%)	273	436	302	394	18.7	95
PMMA/SDS/p-SWCNT-O-APTS (1 wt.%)	279	-	298	391	20.3	96

carbonyl group of PMMA. In addition, the residual amounts of all nanocomposites generally increased with the increase of the filler material.

To investigate the effect of SDS on the thermal stability of nanocomposites, the same nanocomposites were synthesised in SDS medium and the obtained thermograms were shown in Figure 9. T_x, T_{max} and residual amounts calculated from these thermograms were given in Table 2. DTG thermograms of the nanocomposites have been given in the supplementary materials. It is seen that significant changes occur in the thermal stability of nanocomposites synthesised in SDS and non-SDS medium. The samples with the highest thermal stability of PMMA/SDS/p-SWCNT, PMMA/SDS/p-SWCNT-OH and PMMA/SDS/p-SWCNT-O-APTS nanocomposites are PMMA/SDS/p-SWCNT (0.1 wt.%), PMMA/SDS/p-SWCNT-OH (1 wt.%) and PMMA/SDS/p-SWCNT-O-APTS (0.1 wt.%), respectively. The samples with the highest thermal stability for nanocomposites synthesised in an SDS-free medium were nanocomposites containing 0.1 wt.% CNTs. In the medium with SDS, the samples with the highest thermal stability except PMMA/SDS/p-SWCNT-OH (1 wt.%) are PMMA/SDS/p-SWCNT (0.1 wt.%) and PMMA/SDS/p-SWCNT-O-APTS (0.1 wt.%). As can be seen, SDS provides both better dispersion of CNTs in PMMA matrix and increased interaction between CNTs and PMMA. The nanocomposite with the highest thermal stability in SDS medium is PMMA/SDS/p-SWCNT-O-APTS (0.1 wt.%), followed by PMMA/SDS/p-SWCNT-OH (1 wt.%) and PMMA/SDS/p-SWCNT (0.1 wt.%). SDS provided significant increases in both T_{max} and T_x temperatures of the nanocomposites. Increases of 49, 13, 17 and 15°C for T_{max1}, T_{max2}, T₁₀ and T₈₀ temperatures of PMMA/SDS/p-SWCNT-O-APTS (0.1 wt.%) nanocomposite; increases of 41°C, 8°C, 18°C and 30°C for T_{max1}, T_{max2}, T₁₀ and T₈₀ temperatures of

**Figure 9.** TG thermograms of (a) PMMA/SDS/p-SWCNT, (b) PMMA/SDS/p-SWCNT-OH and (c) PMMA/SDS/p-SWCNT-O-APTS nanocomposites.

PMMA/SDS/p-SWCNT-OH (1 wt.%) nanocomposite; and increases of 29, 10, 2 and 33°C for $T_{\max 1}$, $T_{\max 2}$, T_{10} and T_{80} temperatures of PMMA/SDS/p-SWCNT (0.1 wt.%) nanocomposite were obtained relative to PMMA, respectively. Compared to nanocomposites synthesised in SDS-free medium, SDS significantly increased both T_x and T_{\max} temperatures of nanocomposites. For example, for the most thermally stable PMMA/p-SWCNT-OH (0.1 wt.%) nanocomposite in SDS-free medium, $T_{\max 1}$ and $T_{\max 2}$ temperatures increased by 17°C and 5°C, respectively, while for the most thermally stable PMMA/SDS/p-SWCNT-O-APTS (0.1 wt.%) nanocomposite, $T_{\max 1}$ and $T_{\max 2}$ temperatures increased by 49°C and 13°C, respectively. As can be seen, nanocomposites synthesised in SDS medium are approximately 3 times more thermally stable than nanocomposites synthesised in SDS-free medium.

The thermal stability of nanocomposites synthesised with p-SWCNT-OH in SDS-free medium was higher than that of nanocomposites synthesised with p-SWCNT-O-APTS. However, the thermal stability of the nanocomposite prepared with p-SWCNT-O-APTS in SDS medium is higher than other nanocomposites. This result can be explained by the fact that SDS disperses better in the PMMA matrix by reducing the van der Waals attraction

forces among CNTs and creates the appropriate geometry for hydrogen bonding between the carbonyl group of PMMA and the amine group of p-SWCNT-O-APTS. This situation is given in Figure 10. In addition, the nanocomposite with the highest thermal stability among PMMA/SDS/p-SWCNT-OH nanocomposites is PMMA/SDS/p-SWCNT-OH (1 wt.%). This result shows that CNTs, which gain hydrophilic properties by hydroxylation, are homogeneously dispersed in the PMMA matrix by reducing the van der Waals attraction forces between them in the SDS medium and interact more each other.

As seen from Table 2, in general, it was observed that the residual amount of nanocomposites increased with the increase in the amount of filler in the PMMA matrix and the addition of SDS and functionalization. This situation may be due to increasing CNT amount, increasing interaction between CNTs and PMMA with functionalization, and increasing interaction between PMMA and CNT samples with the SDS adding. In literature, ZnO nanostructures were synthesised by hydrothermal method using different molar ratios of CTAB and SDS. The addition of SDS increased both the degradation temperature and the residual amount of ZnO [57].

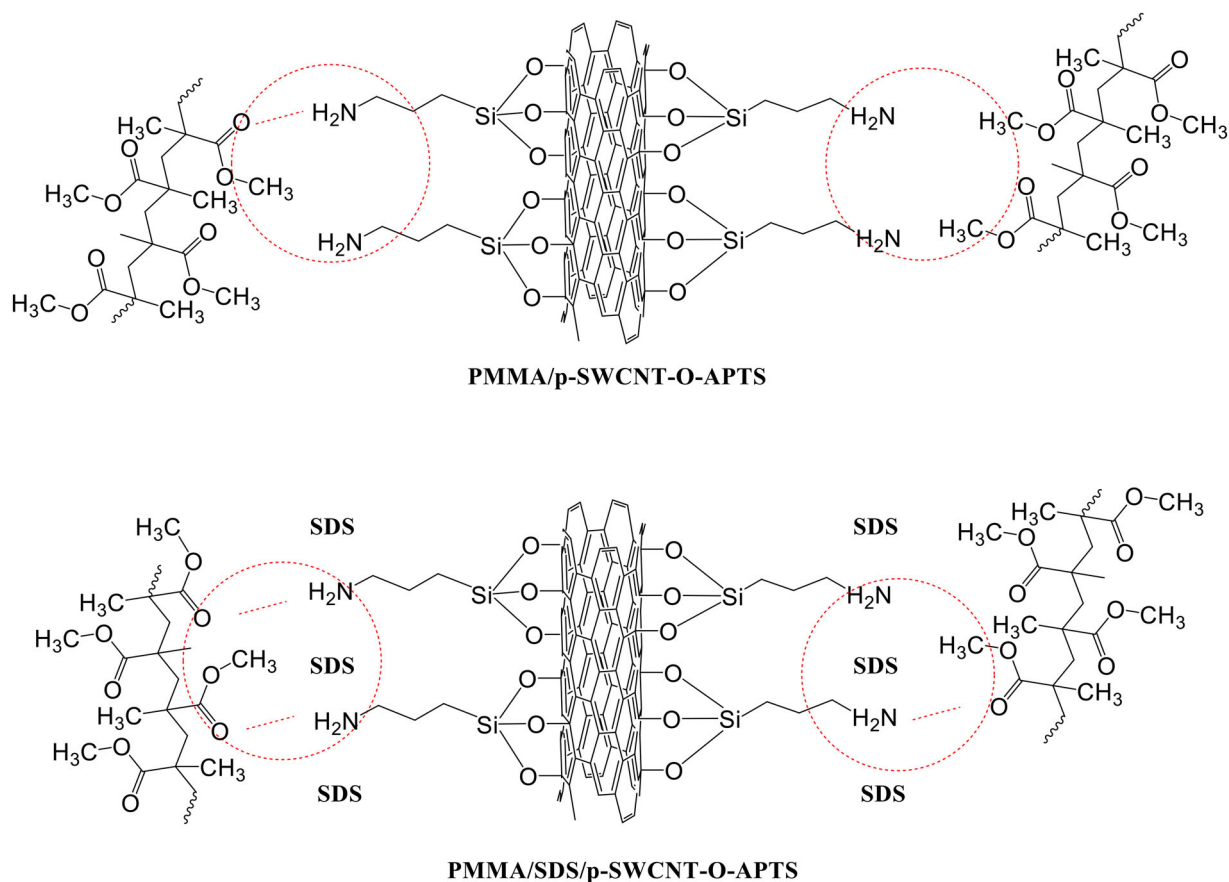


Figure 10. Interactions between the carbonyl group of PMMA and the amine group of p-SWCNT-O-APTS in SDS and SDS-free media.

DSC analysis

The glass transition temperature, T_g , is one of the main distinguishing features of polymeric materials, and this temperature can be determined by DSC analysis. It is the temperature at which the substance loses its glassy properties and begins to acquire viscous properties [58]. In this study, the glass transition temperatures of all nanocomposites prepared in SDS and SDS-free media were measured and compared with the T_g values of PMMA and PMMA/SDS. As can be seen from Table 2, the glass transition temperatures of all nanocomposites increased except PMMA/SDS/p-SWCNT (0.1 wt.%) nanocomposite. Nanocomposites with the highest glass transition temperature were not corresponded to nanocomposites with the highest thermal stability. For example, for nanocomposites prepared in SDS-free medium, the samples with the highest thermal stability were nanocomposites containing 0.1 wt.% CNT, while the samples with the highest glass transition for PMMA/p-SWCNT, PMMA/p-SWCNT-OH and PMMA/p-SWCNT-O-APTS nanocomposites are PMMA/p-SWCNT (1 wt.%) (T_g : 99°C), PMMA/p-SWCNT-OH (0.5 wt.%) (T_g : 105°C) and PMMA/p-SWCNT-O-APTS (0.5 wt.%) (T_g : 100°C).

The samples with the highest glass transition temperature of PMMA/SDS/p-SWCNT, PMMA/SDS/p-SWCNT-OH and PMMA/SDS/p-SWCNT-O-APTS nanocomposites prepared in SDS medium are PMMA/SDS/p-SWCNT (1 wt.%) (T_g : 111°C), PMMA/SDS/p-SWCNT-OH (0.5 wt.%) (T_g : 107°C) and PMMA/SDS/p-SWCNT-O-APTS (1 wt.%) (T_g : 96°C). The nanocomposites with the highest glass transition temperature are the same samples with and without SDS. The increases in the glass transition temperatures of PMMA/SDS/p-SWCNT (1 wt.%), PMMA/SDS/p-SWCNT-OH (0.5 wt.%), and PMMA/SDS/p-SWCNT-O-APTS (1 wt.%) nanocomposites compared to PMMA/SDS are 17°C, 13°C and 2°C, respectively. On the other hand, the increases in the glass transition temperatures of PMMA/p-SWCNT (1 wt.%), PMMA/p-SWCNT-OH (0.5 wt.%) and PMMA/p-SWCNT-O-APTS (1 wt.%) nanocomposites compared to PMMA are 11°C, 17°C and 12°C, respectively. These results show that the addition of SDS to the nanocomposite synthesis medium does not have a significant effect on the glass transition temperatures of the nanocomposites. The highest glass transition temperature increase was obtained as 17°C for PMMA/p-SWCNT-OH (0.5 wt.%) and PMMA/SDS/p-SWCNT (1 wt.%) nanocomposites.

These findings show that PMMA began to fracture at the lower temperature due to the softness of the polymer, while the mechanical fracture of the composite shifted to a higher temperature, suggesting that the p-SWCNT/modified SWCNT samples further restrict the movement of PMMA chains. The surface

modification of SWCNT and the filling ratio affected T_g value of PMMA, resulted in increased stiffness of the composite material and contributed to the mechanical reinforcement [28]. Benlikaya and Alkan examined the glass transition temperatures of PMMA/sepiolite/modified sepiolite nanocomposites and found that the glass transition temperature of PMMA increased in the THF medium and decreased in the acetone medium. T_g value of PMMA was determined as 110°C [56]. In the literature, T_g temperatures of PMMA were measured as 108°C [59], 99.9°C [60] and 96.5°C [27] by different researchers. In this study, T_g values of the PMMA and PMMA/SDS were determined as 88°C and 94°C, respectively. The reason for these variations among the glass transition temperatures of PMMA could also be as a result of the different molecular weights of the polymers used or the specific synthesis methods of PMMA. It can be said that surfaces that provide strong interaction with the polymer, hydrogen bonds at the polymer-substrate interface and SWCNTs dispersed in the polymer with a higher aspect ratio lead to higher T_g temperatures [61].

Conclusions

In this study, by using SWCNTs modified with different functional groups, thermal properties improved PMMA nanocomposites were successfully produced by solvent casting method. In nanocomposites, it was observed that CNT samples were uniformly dispersed in the PMMA matrix, preserved their tubular structure and were in nano size. PMMA/p-SWCNT-OH (0.1 wt.%) nanocomposite is both thermally stable and has a high glass transition temperature. PMMA/SDS/p-SWCNT-O-APTS (0.1 wt.%) nanocomposite is the most thermally stable nanocomposite. These nanocomposites, whose thermal stability and glass transition temperatures have increased, may have more uses in industries such as automobile, aerospace, sports, construction, glass, etc. In addition, the functionalised CNTs may have the potential to be used in improving the thermal properties of other polymers used in industry, and in the energy field, especially in hydrogen and carbon dioxide storage, and in the production of gas sensors.

Disclosure statement

No potential conflict of interest was reported by the author(s).

Funding

The work was supported by Balıkesir University Scientific Research Projects Unit with BAP (Grant number 2.2014.0015) and TÜBİTAK-BİDEB 2211-A National Doctorate Scholarship Program.

Data availability statement

The raw/processed data required to reproduce these findings cannot be shared at this time as the data also forms part of an ongoing study.

ORCID

Mehmet Doğan  <http://orcid.org/0000-0002-3707-0497>

References

- Turhan Y, Alp ZG, Alkan M, et al. Preparation and characterization of poly(vinylalcohol)/modified bentonite nanocomposites. *Micropor Mesoporous Mater.* 2013;174:144–153. doi:10.1016/j.micromeso.2013.03.002
- Turhan Y, Doğan M, Alkan M. Characterization and some properties of poly(vinyl chloride)/sepiolite nanocomposites. *Adv Polym Technol.* 2013;32:E65–E82. doi:10.1002/adv.20271
- Turhan Y, Doğan M, Alkan M. Poly(vinyl chloride)/kaolinite nanocomposites: characterization and thermal and optical properties. *Ind Eng Chem Res.* 2010;49:1503–1513. doi:10.1021/ie901384x
- Doğan M, Yuksel H, Kizilduman BK. Characterization and thermal properties of chitosan/perlite nanocomposites. *Int J Mater Res.* 2021;112:405–414. doi:10.1515/ijmr-2020-8007
- Doğan S, Özcan T, Doğan M, et al. The effects on antioxidant enzymes of PMMA/hydroxyapatite nanocomposites/composites. *Enzyme Microb Technol.* 2020;142:109676. doi:10.1016/j.enzmictec.2020.109676
- Beyli PT, Doğan M, Gündüz Z, et al. Synthesis, characterization and their antimicrobial activities of boron oxide/poly(acrylic acid) nanocomposites: thermal and antimicrobial properties. *Adv Mater Sci.* 2018;18:28–36. doi:10.1515/adms-2017-0025
- Kizilduman BK, Alkan M, Doğan M, et al. Al-pillared-montmorillonite (AlPMt)/poly(methyl methacrylate)(PMMA) nanocomposites: the effects of solvent types and synthesis methods. *Advan Mater Sci.* 2017;17:5–23. doi:10.1515/adms-2017-0012
- Nampoothiri PK, Gandhi MN, Kulkarni AR. Elucidating the stabilizing effect of oleic acid coated LaF₃: Nd³⁺ nanoparticle surface in the thermal degradation of PMMA nanocomposites. *Mater Chem Phys.* 2017;190:45–52. doi:10.1016/j.matchemphys.2016.12.075
- Hu YH, Chen CY. The effect of end groups on the thermal degradation of poly(methyl methacrylate). *Polym Degrad Stab* 2003;82:81–88. doi:10.1016/S0141-3910(03)00165-4
- Iijima S. Helical microtubules of graphitic carbon. *Nature.* 1991;354:56–58. doi:10.1038/354056a0
- Seo DW, Yoon WJ, Park SJ, et al. The Preparation of Multi-walled CNT-PMMA Nanocomposite. *Carbon Sci.* 2006;7:266–270.
- Gürkan İ. Mechanical enhancement of woven composite with vertical aligned carbon nanotubes: investigation of inter laminar shear strength property of nano-stitched laminated composites, [M.Sc. thesis], Istanbul: Istanbul Technical University Graduate School of Science Engineering and Technology, Department of Aeronautics and Astronautics Engineering; 2015.
- Dogan M, Turan M, Beyli PT, et al. Thermal and kinetic properties of poly(vinylacetate)/modified MWCNT nanocomposites. *Fuller Nanotub Carbon Nanostruct.* 2020;29:475–485. doi: 10.1080/1536383X.2020.1860945.
- Yanmaz E, Doğan M, Turhan Y. Effect of sodium dodecyl sulfate on thermal properties of polyvinyl alcohol (PVA)/modified single-walled carbon nanotube (SWCNT) nanocomposites. *Diam Relat Mater.* 2021;115:108359. doi:10.1016/j.diamond.2021.108359
- Allaoui A, Bai S, Cheng HM, et al. Mechanical and electrical properties of a MWNT/epoxy composite. *Compos Sci Technol.* 2002;62:1993–1998. doi:10.1016/S0266-3538(02)00129-X
- Gong X, Liu J, Baskearan S, et al. Surfactant-assisted processing of carbon nanotube/polymer composites. *Chem Mater.* 2000;12:1049–1052. doi:10.1021/cm9906396
- Clayton LM, Sikder AK, Kumar A, et al. Transparent poly(methyl methacrylate)/single-walled carbon nanotube (PMMA/SWNT) composite films with increased dielectric constants. *Adv Funct Mater.* 2005;15:101. doi:10.1002/adfm.200305106
- Park JU, Cho S, Cho KS, et al. Effective in-situ preparation and characteristics of polystyrene-grafted carbon nanotube composites. *Korea-Aust Rheol J.* 2005;17:41–45.
- Du F, Fischer JE, Winey KI. Coagulation method for preparing single-walled carbon nanotube/poly(methyl methacrylate) composites and their modulus, electrical conductivity, and thermal stability. *J Polym Sci, Part B: Polym Phys.* 2003;41:3333–3338. doi:10.1002/polb.10701
- Ayanoglu ZG, Doğan M. Characterization and thermal kinetic analysis of PMMA/modified-MWCNT nanocomposites. *Diamond Relat Mater.* 2020;108:107950. doi:10.1016/j.diamond.2020.107950
- Sumdani G, Islam MR, Yahaya ANA. The effects of anionic surfactant on the mechanical, thermal, structure and morphological properties of epoxy-MWCNT composites. *Polym Bull.* 2019;76:5919–5938. doi:10.1007/s00289-019-02695-1
- Mallakpour S, Abdolmaleki A, Borandeh S. 1-Phenylalanine amino acid functionalized multi walled carbon nanotube (MWCNT) as a reinforced filler for improving mechanical and morphological properties of poly(vinyl alcohol)/MWCNT composite. *Prog Org Coat.* 2014;77:1966–1971. doi:10.1016/j.porgcoat.2014.07.005
- Malikov EY, Muradov MB, Akperov OH, et al. Synthesis and characterization of polyvinyl alcohol based multi-walled carbon nanotube nanocomposites. *Physica E.* 2014;61:129–134. doi:10.1016/j.physe.2014.03.026
- Rafiee R, Pourazizi R. Influence of CNT functionalization on the interphase region between CNT and polymer. *Comp Mater Sci.* 2015;96:573–578. doi:10.1016/j.commat.2014.03.056
- Gupta S, Murthy CN, Prabha CR. Recent advances in carbon nanotube based electrochemical biosensors. *Int J Biol Macromol.* 2018;108:687–703. doi:10.1016/j.ijbiomac.2017.12.038
- Ghosh S, Bachilo SM, Weisman RB. Removing aggregates from single-walled carbon nanotube samples by magnetic purification. *J Phys Chem C.* 2014;118:4489–4494. doi:10.1021/jp411941k

- [27] Kalakonda P, Banne S. Thermomechanical properties of PMMA and modified SWCNT composites. *Nanotechnol Sci Appl.* 2017;Volume 10:45–52. doi:10.2147/NSA.S123734
- [28] Ciobotaru CC, Damian CM, Iovu H. Single-wall carbon nanotubes purification and oxidation. *UPB Sci Bull Ser B Chem Mater Sci.* 2013;75:55–66.
- [29] Punetha VD, Rana S, Yoo HJ, et al. Functionalization of carbon nanomaterials for advanced polymer nanocomposites: a comparison study between CNT and graphene. *Polym Sci.* 2017;67:1–47. doi:10.1016/j.progpolymsci.2016.12.010
- [30] Zniszczoł A, Herman AP, Szymańska K, et al. Covalently immobilized lipase on aminoalkyl-, carboxy- and hydroxy-multi-wall carbon nanotubes in the enantioselective synthesis of solketal esters. *Enzyme Microb Technol.* 2016;87-88:61–69. doi:10.1016/j.enzmictec.2016.02.015
- [31] Yurekli K, Mitchell CA, Krishnamoorti R. Small-angle neutron scattering from surfactant-assisted aqueous dispersions of carbon nanotubes. *J Am Chem Soc.* 2004;126:9902–9903. doi:10.1021/ja047451u
- [32] Cai F, Wang Q, Chen X, et al. Selective binding of Pb²⁺ with manganese-terephthalic acid MOF/SWCNTs: theoretical modeling, experimental study and electro-analytical application. *Biosens Bioelectron.* 2017;98:310–316. doi:10.1016/j.bios.2017.07.007
- [33] Yang CC, Li YJ, Chen WH. Electrochemical hydrogen storage behavior of single-walled carbon nanotubes (SWCNTs) coated with Ni nanoparticles. *Int J Hydrog Energ.* 2010;35:2336–2343. doi:10.1016/j.ijhydene.2010.01.007
- [34] Çalıřır Ü, Çiçek B, Dođan M. Microwave-assisted cross-coupling synthesis of aryl functionalized MWCNTs and investigation of hydrogen storage properties. *Fullerenes Nanotubes Carbon Nanostruct.* 2021. doi:10.1080/1536383X.2021.1913727
- [35] Viřić B, Cohen H, Popovitz-Biro R, et al. Direct synthesis of palladium catalyst on supporting WS₂Nanotubes and its reactivity in cross-coupling reactions. *Chem Asian J.* 2015;10:2234–2239. doi:10.1002/asia.201500271
- [36] Salvo AMP, Parola VL, Liotta LF, et al. Highly loaded multi-walled carbon nanotubes non-covalently modified with a bis-imidazolium salt and their use as catalyst supports. *Chempluschem.* 2016;81:471–476. doi:10.1002/cplu.201600023
- [37] Hajipour AR, Khorsandi Z. Immobilized Pd on (S)-methyl histidinate-modified multi-walled carbon nanotubes: a powerful and recyclable catalyst for mizoroki-heck and suzuki-miyaura C-C cross-coupling reactions in green solvents and under mild conditions. *Appl Organometal Chem.* 2016;30:256–261. doi:10.1002/aoc.3425
- [38] Sundharam S, Choi KH. Fabrication of flexible SWCNT thin films through electrohydrodynamic atomization technique and investigation of their electrical properties. *Mater Lett.* 2014;115:215–218. doi:10.1016/j.matlet.2013.10.088
- [39] Duan G, Zhang C, Li A, et al. Preparation and characterization of mesoporous zirconia made by using a poly (methyl methacrylate) template. *Nanoscale Res Lett.* 2008;3:118–122. doi:10.1007/s11671-008-9123-7
- [40] Derakhshan MS, Moradi O. The study of thermodynamics and kinetics methyl orange and malachite green by SWCNTs, SWCNT-COOH and SWCNT-NH₂ as adsorbents from aqueous solution. *J Ind Eng Chem.* 2014;20:3186–3194. doi:10.1016/j.jiec.2013.11.064
- [41] Liu X, Xu D, Liao C, et al. Development of a promising drug delivery for formononetin: cyclodextrin-modified single-walled carbon nanotubes. *J Drug Deliv Sci Technol.* 2018;43:461–446. doi:10.1016/j.jddst.2017.11.018
- [42] Titus E, Ali N, Cabral G, et al. Chemically functionalized carbon nanotubes and their characterization using thermogravimetric analysis, Fourier transform infrared, and Raman spectroscopy. *JMEPEG.* 2006;15:182–186. doi: 10.1361/105994906X95841.
- [43] Weigel C, Kellner R. FTIR-ATR-spectroscopic investigation of the silanization of germanium surfaces with 3-aminopropyltriethoxysilane. *Anal Chem.* 1989;335:663–668. doi:10.1007/BF01204067
- [44] Yang B, Hu H, Yu Q, et al. Pretreated multiwalled carbon nanotube adsorbents with amine-grafting for removal of carbon dioxide in confined spaces. *RSC Adv.* 2014;4:56224–56234. doi:10.1039/C4RA11271G
- [45] Su F, Lu C, Cnen W, et al. Capture of CO₂ from flue gas via multiwalled carbon nanotubes. *Sci Total Environ.* 2009;407:3017–3023. doi:10.1016/j.scitotenv.2009.01.007
- [46] Gao X, Chorover J. Adsorption of sodium dodecyl sulfate (SDS) at ZnSe and α -Fe₂O₃ surfaces: combining infrared spectroscopy and batch uptake studies. *J Colloid Interface Sci.* 2010;348:167–176. doi:10.1016/j.jcis.2010.04.011
- [47] Wang S, Xie F, Liu G. Direct electrochemistry and electrocatalysis of heme proteins on SWCNTs-CTAB modified electrodes. *Talanta.* 2009;77:1343–1350. doi:10.1016/j.talanta.2008.09.019
- [48] Erinosh MF, Akinlabi ET, Johnson OT. Characterization of surface roughness of laser deposited titanium alloy and copper using AFM. *Appl Surf Sci.* 2018;435:393–397. doi:10.1016/j.apsusc.2017.11.131
- [49] Samyn P, Erps JV, Thienpont H. Relation between optical non-contact profilometry and AFM roughness parameters on coated papers with oil-filled nanoparticles. *Measurement (Mahwah N J).* 2016;82:75–93. doi:10.1016/j.measurement.2015.12.035
- [50] Ghorbani-Vaghei R, Hemmati S, Hashemi M, et al. Diethylenetriamine-functionalized single-walled carbon nanotubes (SWCNTs) to immobilization palladium as a novel recyclable heterogeneous nanocatalyst for the suzuki-miyaura coupling reaction in aqueous media. *C R Chim.* 2015;18:636–643. doi:10.1016/j.crci.2014.10.010
- [51] Zeng WR, Li SF, Chou WK. Chemical kinetics on thermal oxidative degradation of PMMA. *Chin J Chem Phys.* 2003;16:64–68.
- [52] Grassie N, Scott G. *Polymer degradation and stabilization.* Cambridge: Cambridge University Press; 1985.
- [53] Nikolaidis AK, Achilias DS. Thermal degradation kinetics and viscoelastic behavior of poly(methyl methacrylate)/organomodified montmorillonite nanocomposites prepared via In situ bulk radical polymerization. *Polymers (Basel).* 2018;10:491. doi:10.3390/polym10050491
- [54] Gao Z, Kaneko T, Hou D, et al. Kinetics of thermal degradation of poly(methyl methacrylate) studied with the assistance of the fractional conversion at the maximum reaction rate. *Polym Degrad Stab* 2004;84:399–403. doi:10.1016/j.polymdegradstab.2003.11.015
- [55] Kausar A. Hybrid polymer composite materials. *Hybrid Polym Comp Mater.* 2017: 115–132. doi:10.1016/B978-0-08-100787-7.00005-6

- [56] Benlikaya R, Alkan M. Influence of constituents on thermal properties of polymethacrylate derivatives–clay materials. *Polym Compos.* 2011;32:615–628. doi:10.1002/pc.21083
- [57] Ramimoghadam D, Hussein MZB, Taufiq-Yap YH. The effect of sodium dodecyl sulfate (SDS) and cetyltrimethylammonium bromide (CTAB) on the properties of ZnO synthesized by hydrothermal method. *Int J Mol Sci.* 2012;13:13275–13293. doi:10.3390/ijms131013275
- [58] Hou PX, Liu C, Cheng HM. Purification of carbon nanotubes. *Carbon N Y.* 2008;46:2003–2025. doi:10.1016/j.carbon.2008.09.009
- [59] Porter CE, Blum FD. Thermal characterization of PMMA thin films using modulated differential scanning calorimetry. *Macromolecules.* 2000;33:7016–7020. doi:10.1021/ma000302l
- [60] Elshereksi NW, Mohamed SH, Arifin A, et al. Thermal Characterisation of Poly(Methyl Methacrylate) Filled with Barium Titanate as Denture Base Material. *J Phys Sci.* 2014;25:15–27.
- [61] Bhattacharya M. Polymer nanocomposites—a comparison between carbon nanotubes, graphene, and clay as nanofillers. *Materials (Basel).* 2016;9:262, doi:10.3390/ma9040262